

Reactor and Nuclear Systems Division

Direct Measurement of Plutonium in Spent Fuel with X-ray Fluorescence

Catherine Romano, Allisa Stafford,* Alexander Solodov, Michael Ehinger

*Texas A&M University, College Station, TX 77843

December 2010

Prepared for
Office of Dismantlement and Transparency (NA-241)
U.S. Department of Energy

Funded by
Next Generation Safeguard Initiative
U.S. Department of Energy

Prepared by
OAK RIDGE NATIONAL LABORATORY
P.O. Box 2008
Oak Ridge, Tennessee 37831-6283
managed by
UT-BATTELLE, LLC
for the
U.S. DEPARTMENT OF ENERGY
under contract DE-AC05-00OR22725

CONTENTS

LIST OF ACRONYMS	II
1. INTRODUCTION.....	1
1.1 Next Generation Safeguards Initiative Spent Fuel Research	1
1.2 Overview of the XRF Measurement.....	1
2. SPENT FUEL XRF MEASUREMENTS.....	2
2.1 History	2
2.2 The XRF Source.....	3
2.3 Spent Fuel Characteristics.....	3
2.4 Experimental Setup and Procedure	5
2.5 Spectrum Analysis.....	6
3. SPENT FUEL XRF SIMULATIONS	8
3.1 Simulation Goals	8
3.2 Simulation Methodology	8
3.2.1 TransLAT Calculation	9
3.2.2 The Beta and Gamma Source	9
3.2.3 Simulation Geometry and Compton Effects.....	10
3.2.4 Simulation Results	11
3.3 Simulated Data Analysis.....	12
4. CONCLUSIONS.....	14
5. REFERENCES.....	15

LIST OF ACRONYMS

ADEPT	Advanced Diagnostics and Evaluation Platform
BWR	boiling water reactor
FP	fission fragment
HPGe	high purity germanium
IAEA	International Atomic Energy Agency
IFEL	Irradiated Fuel Examination Laboratory (at ORNL)
LWR	light water reactor
MOX	mixed oxide
NDA	nondestructive assay
NGSI	Next Generation Safeguards Initiative
ORNL	Oak Ridge National Laboratory
Pu	plutonium
PWR	pressurized water reactor
SNF	spent nuclear fuel
TMI	Three Mile Island
U	uranium
XRF	X-ray fluorescence

1. INTRODUCTION

1.1 Next Generation Safeguards Initiative Spent Fuel Research

In June 2007, the Department of Energy concluded a study on advanced safeguards approaches (ASA-100) for new reprocessing facilities. The statement of needs in the conclusions and recommendations section of the final report for that study included the following [1]:

Develop a method to accurately measure the plutonium (Pu) and actinide content in spent LWR fuel and metallic fast-reactor fuel for the random verification of the spent fuel receipts, and to provide an analytical basis for estimating shipper/receiver differences in a timely manner. It is expected that this method should be capable of detecting “partial-defects” in accordance with current IAEA criteria, i.e. approximately $\pm 5\%$ total Pu.

In March 2009, the Next Generation Safeguards Initiative (NGSI) of the National Nuclear Security Administration initiated an effort to address the needs identified in the ASA-100 report, including the need to quantify the mass of Pu in spent nuclear fuel assemblies for safeguards purposes [2]. The NGSI Spent Fuel Effort identified 14 nondestructive assay (NDA) techniques for use in detecting elemental Pu mass and/or possible diversions. Most of the measurement techniques currently being investigated are neutron based; however, X-ray fluorescence (XRF) measurements also are being considered. Measurements of the self-induced XRF peaks of uranium (U) and Pu provide a direct measurement of Pu in spent nuclear fuel (SNF). The ratio of the areas under the X-ray peaks from the Pu and U might be correlated to the total Pu/U ratio in the spent fuel that is to be verified by destructive analysis.

1.2 Overview of the XRF Measurement

U and Pu X-rays have been measured previously in small aliquots of spent fuel dissolutions [3,4]. However, only limited measurements of the Pu K X-rays in solid spent fuel have been conducted. The first published observation of the 103.7 keV Pu X-ray from spent fuel was by C. Rudy et al. in 1998 [5]. This was a measurement of BN-350 fast breeder reactor spent fuel that had been cooling for 5–10 years prior to measurement. The ratio of the 103.7 keV peak area to the continuum was low, and the peak areas had large errors that could be attributed to the detector being used for this measurement was not specifically designed to measure these X-rays.

The direct measurement of X-ray lines from passively induced XRF has been achieved for the first time in standard light water reactor (LWR) and mixed oxide (MOX) spent fuel at Oak Ridge National Laboratory (ORNL) [6,7,8]. In support of the XRF measurements, MCNP5 simulations were completed at Texas A&M University [9]. The XRF simulations indicated that the ratio of the Pu to U X-ray peak areas have a good straight line correlation to the Pu/U content at the outer edge of the fuel. Destructive analysis will provide a correlation of the measured peak ratios to the total Pu content within the fuel and will be used to verify measurements and simulations. Since the Compton scattering background is large, efforts are being made to optimize the experimental configuration to reduce measurement times with the goal of developing a deployable verification system.

XRF techniques by themselves may be insufficient for complete characterization of SNF assemblies. However, because XRF measures the Pu in the fuel directly, it can be a powerful

verification measurement when combined with other methods that assay an entire assembly. The benefit of XRF is that the detector “sees” only a single fuel pin without interference from the entire assembly due to the low energy of the X-rays. This avoids the complication of deconvoluting a signal produced by self-shielding, absorption, and multiplication within an assembly. With the use of appropriate reactor physics models and algorithms, the pin measurement can then be extrapolated to the entire assembly to validate burn-up and Pu content. Forensic crossover applications give these measurements and simulations additional importance.

The XRF measurement is intended for use by safeguards professionals as part of an integrated strategy to determine the elemental Pu. The goals of this XRF work are as follows:

1. optimize an XRF detection system;
2. correlate XRF measurement and simulation results to destructive analysis in order to determine total Pu/U in SNF based on measured ratios;
3. develop a passive, lightweight, and portable system to complement assembly measurements; and
4. leverage the ability to isolate a single pin.

In short, an XRF detector as called out in the integrated strategy is a lightweight, inexpensive instrument that can quantify fissile content in spent fuel and can be deployed to facilities for safeguards purposes.

2. SPENT FUEL XRF MEASUREMENTS

2.1 History

Several measurement campaigns were performed in the hot cells at the Irradiated Fuel Examination Laboratory (IFEL) at ORNL (Table 1). The measurements performed in May 2008 failed to produce a viable Pu X-ray measurement due to the large Compton continuum from gamma-ray interactions in the fuel, detector, shielding, and other materials. The detector arrangement was simulated with MCNP5 [10], and the simulations suggested possible changes to the detector shielding which would decrease the Compton continuum by an order of magnitude. In July 2008, modifications to the detector shielding, performed based on the results from these simulations, resulted in a measurable Pu X-ray signal. In January 2009, the detector and the experimental arrangement were modified to further increase the signal-to-noise ratio. Thus, Pu/U X-ray ratios were shown to be measurable for LWR spent fuels with burn-ups ranging from 30 to 70 GWd/tU. The description in the remainder of this paper is limited to the January 2009 measurement campaign, which comprises a burn-up range from 25 to 50 GWd/tU.

Table 1. XRF measurements conducted on the various fuels at ORNL

Date	Fuel Measured	Number of XRF Measurements
Jul 2008	North Ana	9
Jan 2008	TMI	9
Sep 2009	Catawba	16
Oct 2009	Calvert Cliffs	2
Nov 2009	Catawba	11
Aug 2010	TMI, Limerick	10

2.2 The XRF Source

LWR spent fuel contains, by weight, approximately 1% Pu and 3% fission products with the remainder U [11]. The fission products produce an intense gamma-ray field that obscures the Pu gamma rays. The radioactive decay of the spent fuel, however, will induce fluorescence in the U and Pu, producing K X-rays. These X-rays show promise of being a useful NDA signature of the Pu-to-U ratio in the spent fuel.

The U and Pu K X-rays range from about 94 to 120 keV. The energy and relative intensities of these X-rays are shown in Table 2. Since the bulk of the spent fuel is U, the Pu X-rays, with energy similar to that of the U X-rays, will likely be obscured. However, the 103.7 keV $K_{\alpha 1}$ X-ray of Pu is relatively well separated from the U X-rays and is measureable in spent fuel.

Table 2. Uranium and plutonium X-ray data [12]

X-Ray	Energy (keV)		Relative Intensity (%)	
	Uranium	Plutonium	Uranium	Plutonium
$K_{\alpha 1}$	98.44	103.76	100	100
$K_{\alpha 2}$	94.67	99.55	61.9	62.5
$K_{\beta 1}$	111.30	117.26	22.0	22.2
$K_{\beta 2}$	114.50	120.60	12.3	12.5
$K_{\beta 3}$	110.41	116.27	11.6	11.7

2.3 Spent Fuel Characteristics

Several types of spent fuel that have a wide range of initial enrichments, burn-up, and cooling times are available for measurement at IFEL. Table 3 provides some properties of the measured fuel, which were in segments approximately 1 m long and contained in steel shipping tubes.

Table 3. Select properties of the spent fuel

Reactor	Type	Initial Enrichment (%)	Burn-up	Discharged
TMI	PWR	4.00	49–50.9	1997
Surry	PWR	3.11	36	1981
Limerick	BWR	3.95	57	1998
North Ana	PWR	4.199	67	2004
Calvert Cliffs	PWR	3.038	41.8	1982
Catawba*	PWR	2.42–4.99**	39.7–47.3	2008

* MOX fuel

** Initial plutonium enrichment

The measurements described in this report were performed with rod D5 from assembly NJ05YU from TMI-1. This rod had an average burn-up of approximately 50 GWd/tU. The characteristics of the rod and assembly are given in Table 4. The rod had been cut previously into segments of varying lengths and packaged into stainless steel shipping tubes with a thickness of approximately 0.16 cm. The rods were measured while still in the shipping tubes, which was found to increase the Compton background. Subsequent measurements were completed without the shipping tubes, and the data is still under analysis.

Table 4. Characteristics of TMI-1 spent fuel rod D5 from assembly NJ05YU [13]

Parameter	Value
Assembly and reactor data	
Design	B&W PWR
Lattice geometry	15x15
Rod pitch (cm)	1.4427
Number of fuel rods	208
Number of guide tubes	16
Number of instrumentation tubes	1
Assembly pitch (cm)	21.8110
Fuel rod data	
Fuel material	UO ₂
Fuel pellet density (g/cm ³)	10.196
Fuel pellet diameter (cm)	0.9362
Clad material	Zircaloy-4
Clad inner diameter (cm)	0.9576
Clad outer diameter (cm)	1.0922
Guide/instrument tube data	
Guide/ instrumentation tube material	Zircaloy-4
Guide tube inner diameter (cm)	1.2649
Guide tube outer diameter (cm)	1.3462
Instrumentation tube inner diameter (cm)	1.1201
Instrumentation tube outer diameter (cm)	1.2522

2.4 Experimental Setup and Procedure

The spent fuel rod segments were placed in the IFEL hot cell at ORNL. The fuel segments were removed from their shipping tubes and placed, one at a time, onto the Advanced Diagnostics and Evaluation Platform (ADEPT), which is a device specifically designed for use in examination of SNF. The ADEPT rod positioning system is capable of dimensionally measuring full-length fuel rods and precisely moving the fuel rod such that its entire length can pass in front of a collimated port hole through the hot-cell wall. The ADEPT rod positioning system is shown in Figure 1. The experimental setup inside the hot cell is shown in Figure 2, including the ADEPT system with a shield that collimates gamma rays into a thin beam projecting through the hot cell wall. The collimator is 65.75 in. long, and the hot cell walls are 36.0 in. thick. The collimator extends 27.5 in. into the hot cell and is 8 in. from the fuel rod. The collimator extends 12.25 in. further outside the hot cell wall. The collimator has a rectangular window that is fixed at 0.75 in. vertically and is adjustable up to 0.25 in. horizontally.

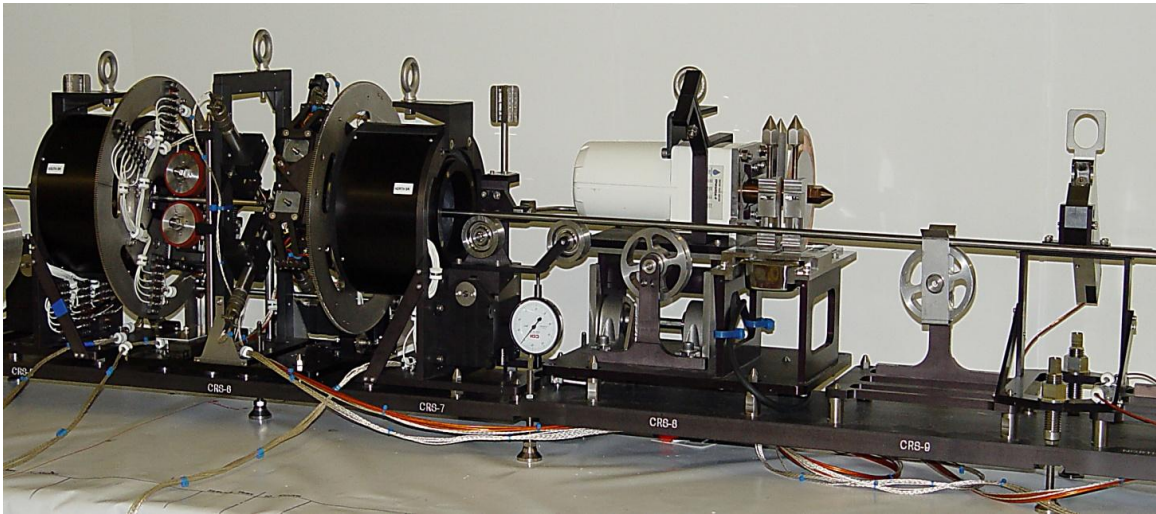


Figure 1. ADEPT system for precisely moving spent fuel.

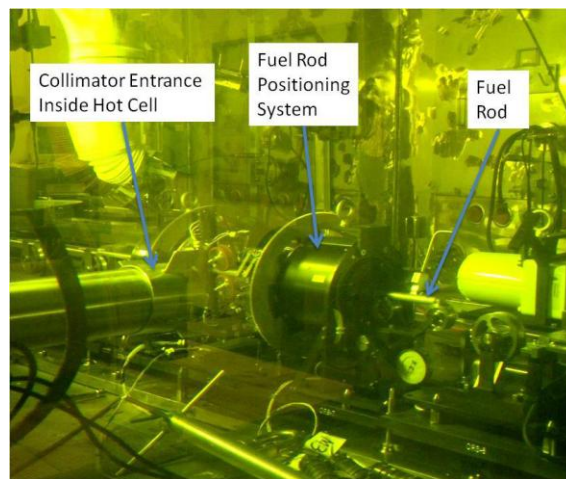


Figure 2. Collimator, fuel rod, and ADEPT rod positioning system arrangement inside hot cell.

A Canberra Model GL0515R planar detector, which is a low-energy germanium detector, was placed directly against the collimator extension. The tungsten collimator on the detector was removed, and no shielding was placed around the detector, which corresponds to the detector front face being 73.75 in. from the fuel rod. Gamma-ray spectra were collected from various positions along the fuel rod, with the majority of positions being near the top of the fuel rod (where the fuel burn-up changed the most with change in distance from the end of the rod). Counting times varied from 1 to 16 hours. The detector dead times varied from 6 to 16% depending on the rod location. With the detector and collimator in this arrangement and using 4 to 16 hour count times, the 103.7 keV X-ray peak from Pu was clearly visible as shown in the example spectrum in Figure 3.

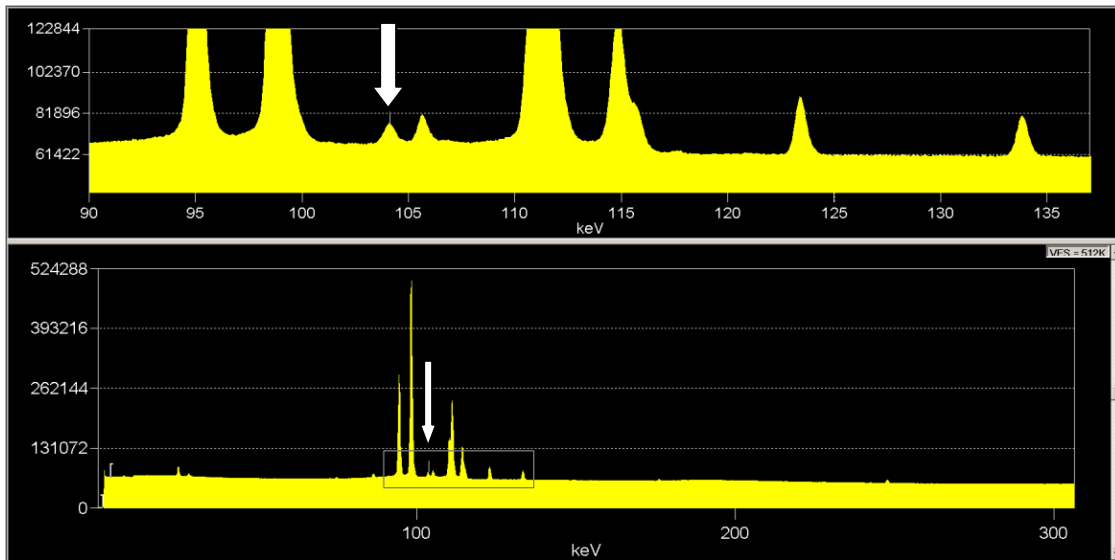


Figure 3. Measured spectra from TMI spent fuel rod D5.
The Pu X-ray peak at 103.7 keV is indicated by the arrows.

2.5 Spectrum Analysis

The measured spectra were analyzed using Canberra's GENIE 2000 interactive peak fit. An example peak fit is shown in Figure 4. As can be seen, there is a ^{155}Eu gamma peak at 105.3 keV that is near to the Pu $\text{K}_{\alpha 1}$ 103.7 keV X-ray peak, but these peaks are easily separable using a high resolution detector.

The spectra were analyzed to acquire count rates for the U K X-ray at 98.4 keV, the Pu K X-ray at 103.7 keV, the ^{134}Cs gamma ray at 604 keV, and the ^{137}Cs gamma ray at 661 keV. The ratio of $^{134}\text{Cs}/^{137}\text{Cs}$ is an indicator of fuel burn-up [9]. The measured Pu/U K X-ray ratio was then plotted versus the measured $^{134}\text{Cs}/^{137}\text{Cs}$ gamma-ray ratio and is shown in Figure 5. As can be seen, a strong correlation between Pu/U X-ray ratio and $^{134}\text{Cs}/^{137}\text{Cs}$ gamma-ray ratio is found, which indicates that the Pu/U peak ratio should correlate linearly with burn-up as well.

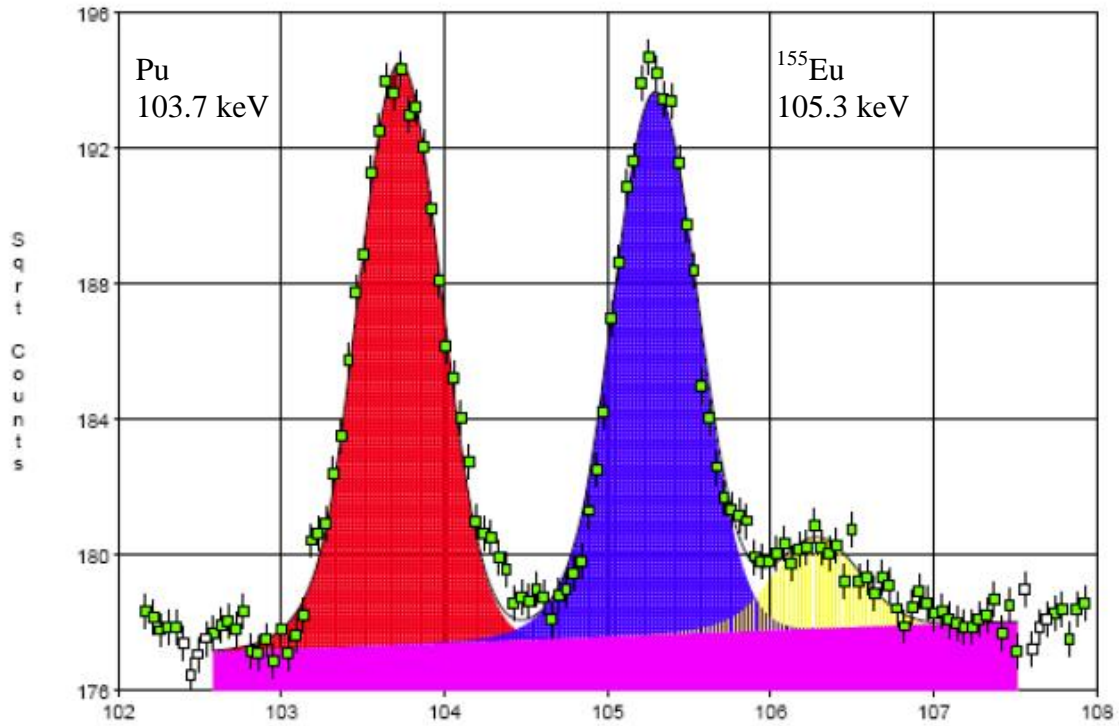


Figure 4. Example peak fit for Pu X-ray peak at 103.7 keV using the GENIE 2000 interactive peak fit.

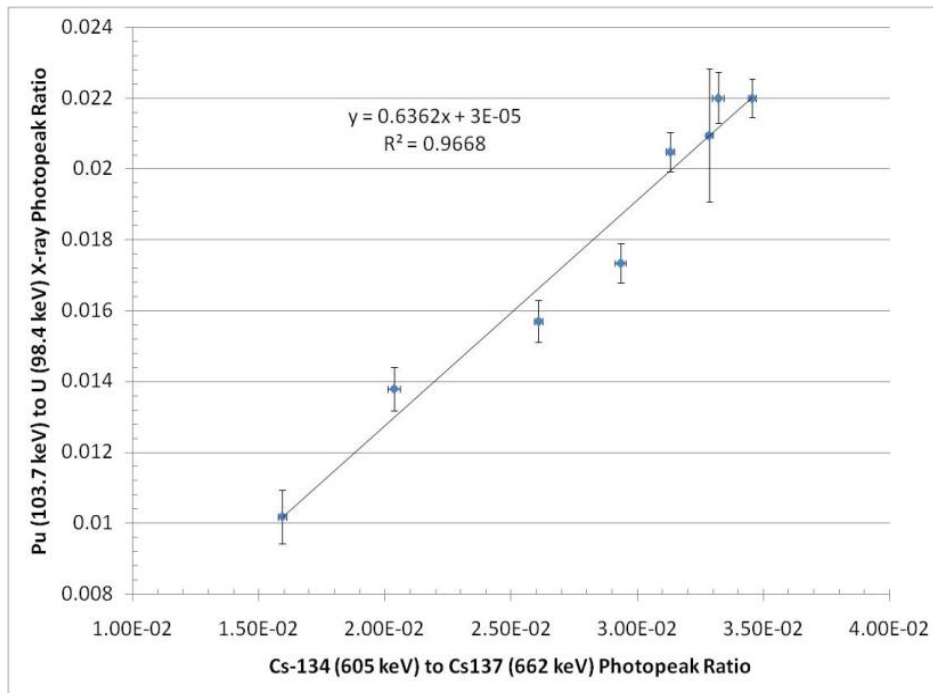


Figure 5. Measured Pu/U X-ray ratio versus measured $^{134}\text{Cs}/^{137}\text{Cs}$ gamma-ray ratio for TMI fuel rod D5.

3. SPENT FUEL XRF SIMULATIONS

3.1 Simulation Goals

MCNP5 simulations of the XRF experiment were conducted at Texas A&M University [9]. The goal of the simulations was to understand the source of XRF from spent fuel and how these relate to the isotopic inventory distributions in the fuel as well as to determine the sources of noise and related error. The simulations ultimately aided in evaluating the measured data and helped direct experimental measurement campaigns. Eventually, the simulations can be used to design an instrument to be implemented in a forensics or safeguards application.

3.2 Simulation Methodology

Destructive analysis of the samples measured from rod D5 has yet to be performed at the time of writing this paper. Thus to examine the feasibility of this technique, simulations were used to relate the measured $^{134}\text{Cs}/^{137}\text{Cs}$ gamma-ray ratio to burn-up and the expected Pu/U content in the spent fuel. The simulation methodology is shown in Figure 6. First, a two-dimensional TransLAT simulation [14] was used to determine the expected fuel isotopics as a function of fuel burn-up and radial position in the fuel pin. Based on the isotopic distributions, the beta source term and gamma source term were calculated using ORIGEN and MCNP5, and the X-ray fluorescence source term was determined. MCNPX was then used to transport the X-ray source to the detector to produce particle tracks and a pulse height spectrum.

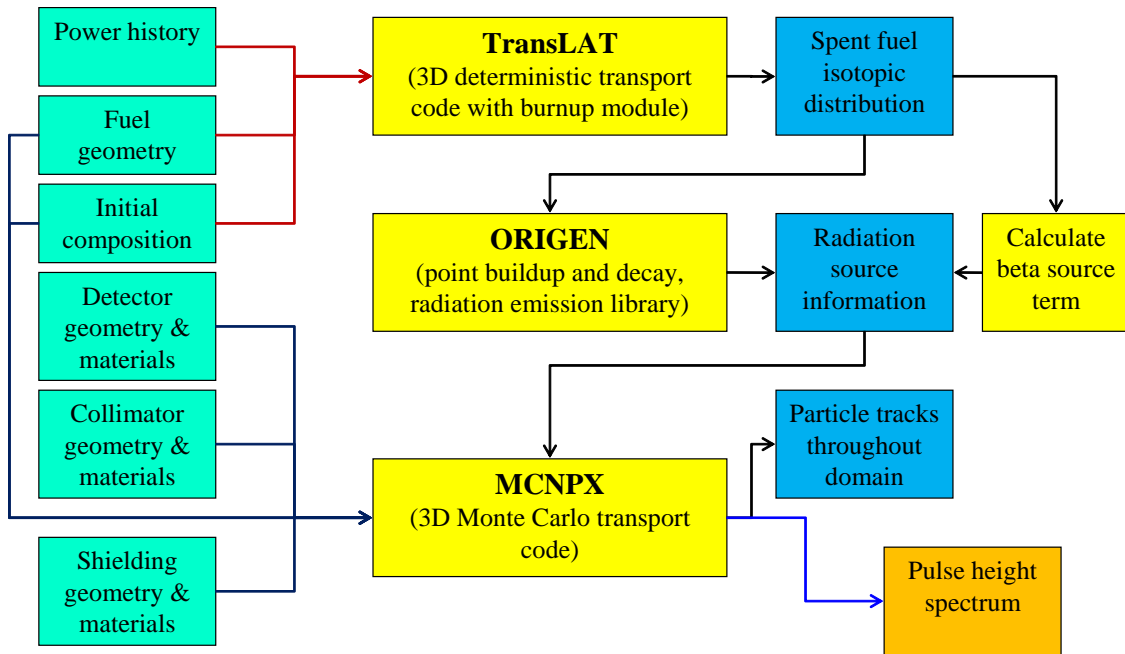


Figure 6. The simulation methodology for the XRF measurement of a fuel pin in the hot cell at ORNL.

3.2.1 TransLAT Calculation

The TransLAT simulation included 20 radial fuel regions in the fuel pin where the radius of each region varied as a function of the mean free path of the X-rays given by

$$r_i = R \frac{(1 - e^{-\Sigma_a i})}{(1 - e^{-\Sigma_a N})} , \quad (1)$$

where r_i is the radius of section i , R is the radius of the fuel, Σ_a is the absorption cross section of the X-ray, and N is the number density of the fuel. The fuel pin was burned from 0 to 70 GWd/tU and included the declared decay time for the TMI-1 D5 rod from time of discharge to time of measurement. As shown in Figure 7, the Pu and fission products are more highly concentrated on the outer edges of the fuel. The U concentration changes only slightly as a function of position within the pin, but the Pu concentration is almost a factor of 5 higher on the outer surface of the pin than in the center of the pin. In contrast, the $^{134}\text{Cs}/^{137}\text{Cs}$ atom ratio changes only slightly (about 5–10%) as a function of radial position in the pin. Consequently, there is only minimal attenuation of the 605 and 661 keV gamma rays from ^{134}Cs and ^{137}Cs regardless of where in the pin they are produced.

3.2.2 The Beta and Gamma Source

The XRF is induced in the Pu and U in spent nuclear fuel by beta and gamma radiation. Simulations were used to understand the strength of XRF induced by each of these sources. The beta source used for simulations was a 317 energy group beta spectrum from 0 to 3.17 MeV obtained from Lawrence Berkeley National Laboratory. A separate energy spectrum was calculated for each radial region. The gamma spectrum obtained using ORIGEN includes 2100 nuclides with gammas emitted from alpha emission, beta emission, electron capture, and others, resulting in 115,000 individual photon lines.

For burn-ups from 30 to 67 GWd/MTU and cooling times from 4.2 to 13.3 years, beta decay accounts for only 14% of the total X-ray signal [15]. The beta simulations are very time consuming. For 10^8 particle histories, computer run times were 5217 minutes with 7% uncertainty for the beta calculation and only 172 minutes with 1–2% uncertainty for the gamma calculation. It was therefore decided to omit the beta source in future calculations of peak ratios.

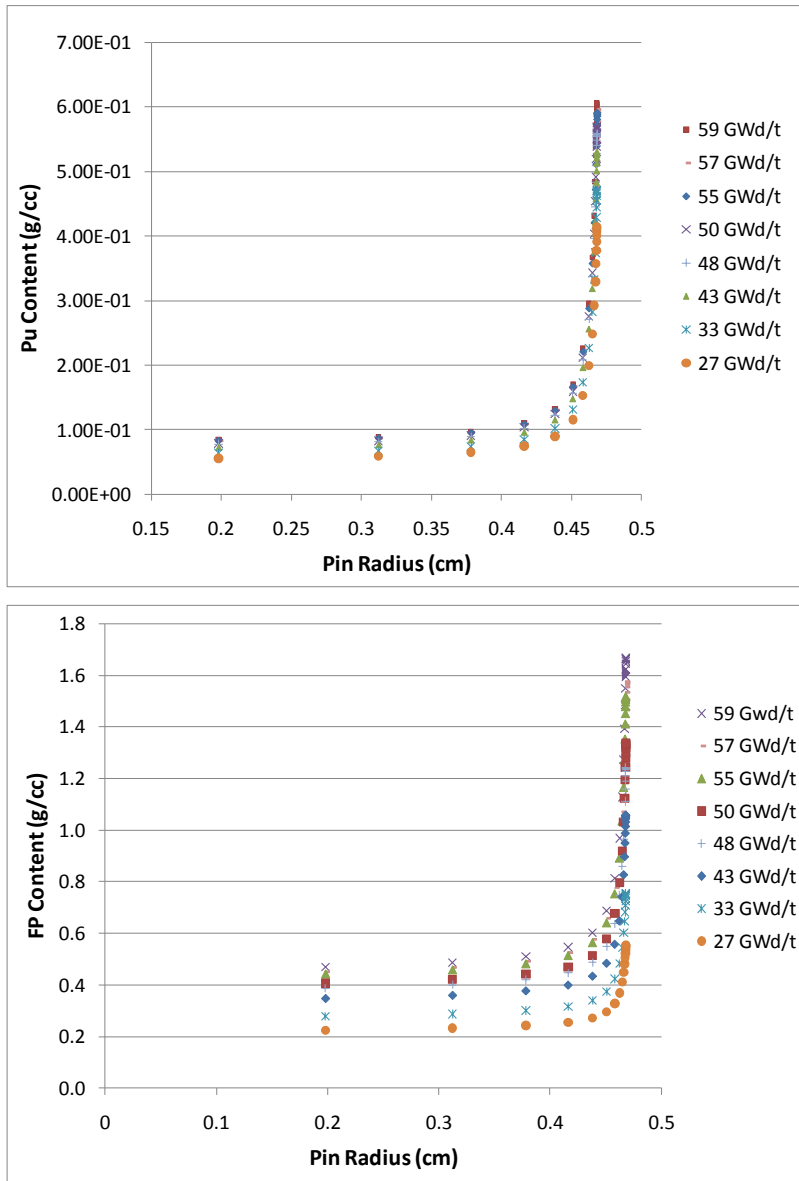


Figure 7. Radial distribution of Pu and fission fragments (FP) as a function of radius calculated using TransLAT.

3.2.3 Simulation Geometry and Compton Effects

The simulation geometry consisted of a 65.75 in. collimator with a 12.25 in. extension piece. The opening in the collimator is 0.25 in. by 0.75 in. A high purity germanium (HPGe) detector was modeled based on detector specification sheets, and exterior details were excluded. The setup is shown in Figure 8.

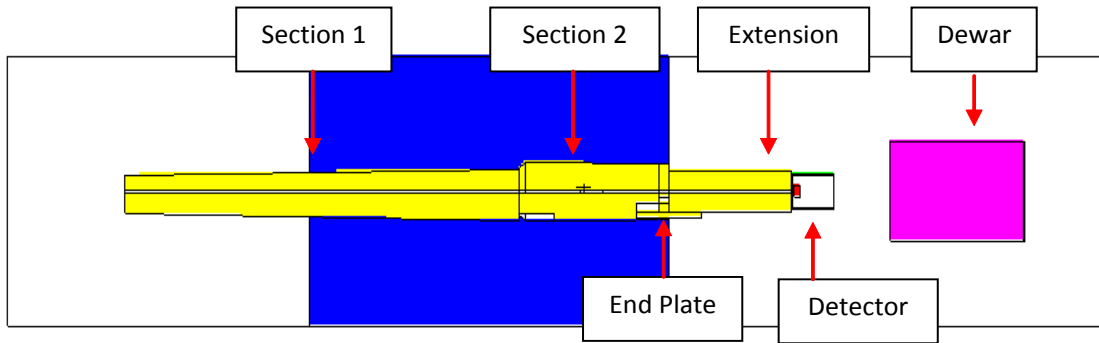


Figure 8. Geometry of the collimator that extends from the fuel, through the hot cell wall, and to the detector.

The Compton scattering background needs to be minimized to allow better discernment of the Pu X-ray peak. An examination was conducted to determine the origin of the largest source of Compton scattered gammas. The conclusion was that the majority of the Compton background originated in the fuel, followed by the shipping tube, the cladding, the detector can, and the collimator end. A titanium collimator attached to the detector itself also produced Compton scattering and was removed prior to the simulation. The shipping tube was also removed based on this simulation. Additional improvements could still be made by redesigning the collimator end to reduce Compton scattering.

3.2.4 Simulation Results

The resulting simulated X-ray spectrum is shown in Figure 9. When compared with the measured spectrum, the simulated spectrum shows some errors. The X-rays peaks in the simulated spectrum are 0.5 keV greater than the actual energies due to an error in the MCNPX code, and the 110 and 111 keV X-ray peaks are combined. In addition, there are some fission product concentration discrepancies in the peak on the right. It was also determined that the 98 keV U X-ray has many other peaks under it that contribute to the peak area. Therefore, it is recommended that the 94 keV U peak be used in the Pu/U ratio.

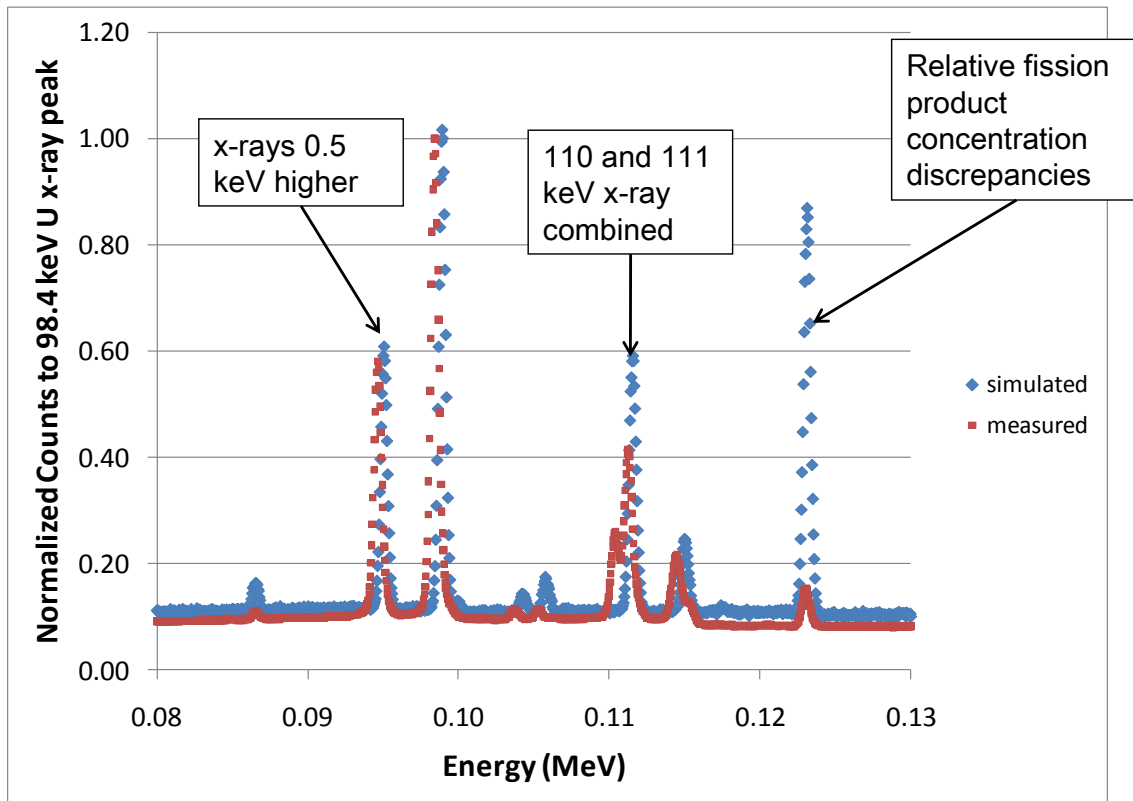


Figure 9. Comparison of the simulated and measured XRF spectrum.

3.3 Simulated Data Analysis

The calculated average Pu/U atom ratio in the fuel pin versus the $^{134}\text{Cs}/^{137}\text{Cs}$ atom ratio in the pin is shown in Figure 10. When correlated to the measured $^{134}\text{Cs}/^{137}\text{Cs}$ ratio from Figure 5, we find that the Pu/U atom ratio predicted using Figure 6 is very low. For example, a measured $^{134}\text{Cs}/^{137}\text{Cs}$ ratio of 0.025 would correspond to a measured Pu/U ratio of approximately 0.016 using Figure 7. However, the same $^{134}\text{Cs}/^{137}\text{Cs}$ ratio of 0.025 would correspond to a Pu/U ratio of 0.003 from Figure 10. The measured Pu/U X-ray ratio is heavily influenced by the concentration of Pu on the outer surface of the fuel pin due to the strong attenuation of the 103.7 keV X-rays in the fuel.

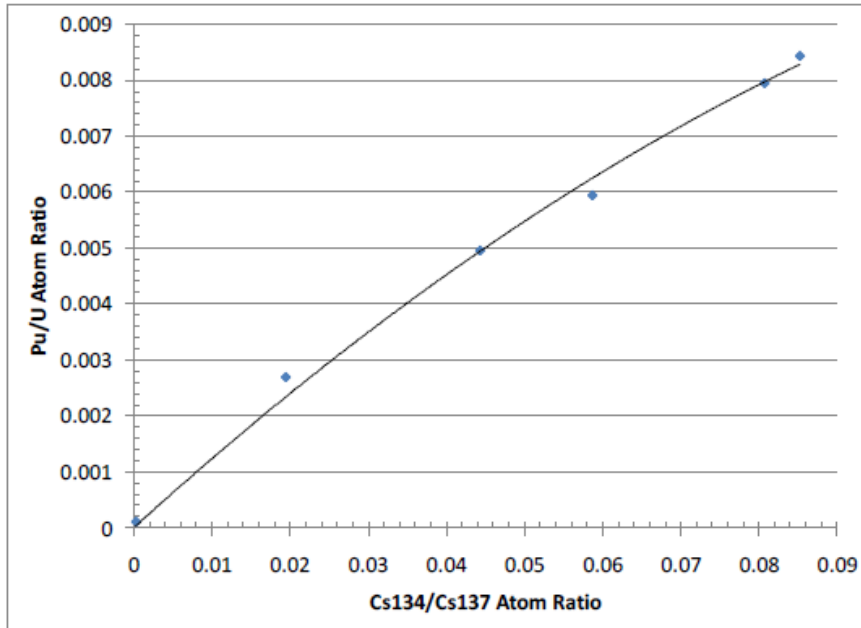


Figure 10. Calculated volumetrically averaged Pu/U atom ratio versus $^{134}\text{Cs}/^{137}\text{Cs}$ atom ratio for TMI fuel rod D5.

Figure 7 shows the Pu concentration that was calculated as a function of radial position in the fuel for several burn-ups. The TransLAT calculated Pu/U atom ratio on the surface of the fuel pin was correlated to the average $^{134}\text{Cs}/^{137}\text{Cs}$ atom ratio for the pin. This correlation was then used to infer the Pu/U atom ratio at the surface of the pin from the measured $^{134}\text{Cs}/^{137}\text{Cs}$ gamma-ray ratio. A plot of the measured Pu/U X-ray ratio versus the inferred Pu/U atom ratio at the surface of the pin is shown in Figure 11. The plot shows that the measured X-ray ratio is a good measure of the Pu/U concentration at the surface of the pin. The Pu/U concentration at the surface of the pin can be directly related to the average Pu/U ratio for the entire pin given knowledge of the pin dimensions, which typically would be known. This correlation is displayed in Figure 12. Thus, it is feasible to measure the Pu/U X-ray ratio and $^{134}\text{Cs}/^{137}\text{Cs}$ gamma-ray ratio for LWR spent fuel pins with burn-ups from 30 to 70 GWd/tU and use this data to determine the Pu/U atom ratio in the pin. This correlation could be validated from the results of the destructive analysis.

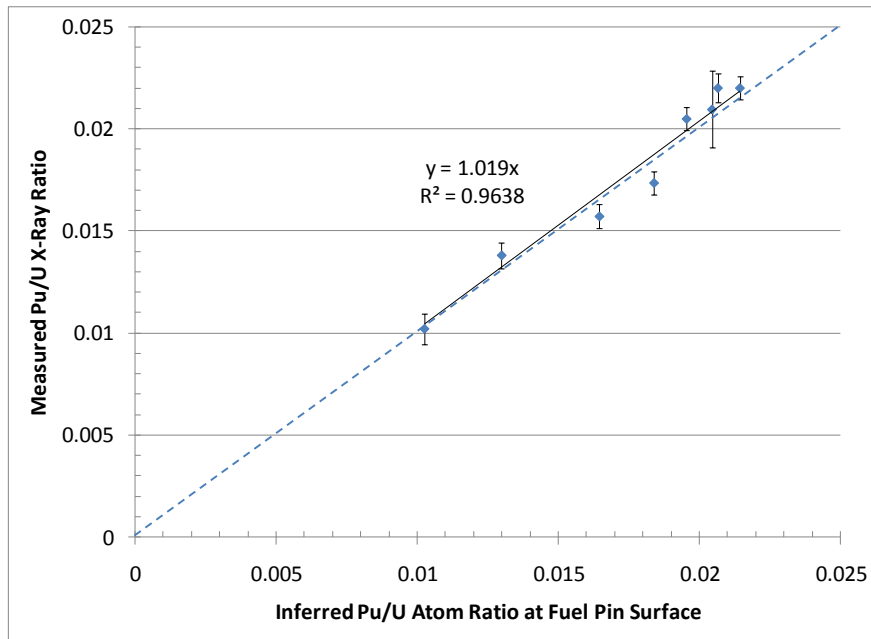


Figure 11. Measured Pu/U X-ray ratio versus Pu/U atom ratio at fuel pin surface inferred from the measured $^{134}\text{Cs}/^{137}\text{Cs}$ gamma-ray ratio.

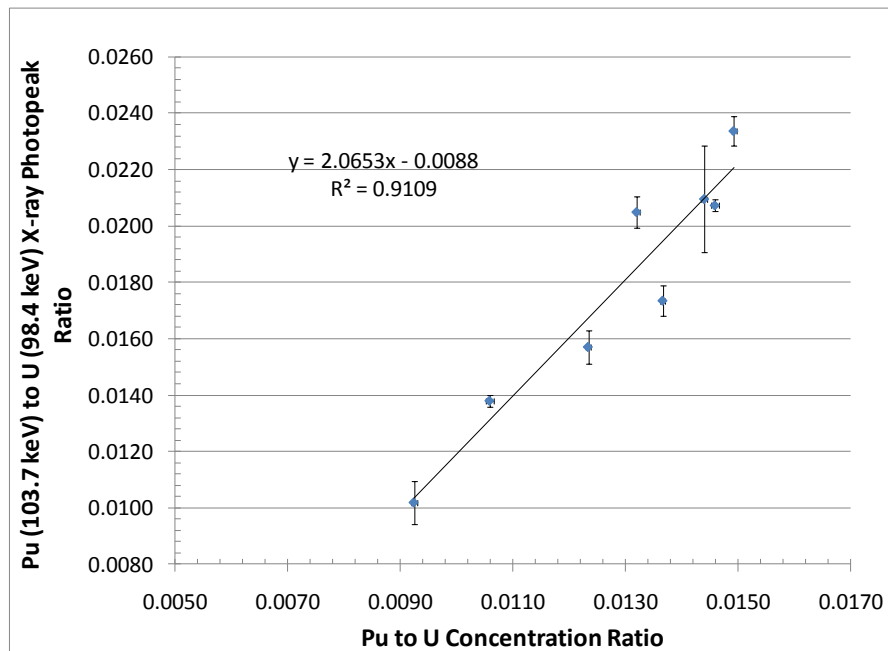


Figure 12. Correlation between measured Pu/U ratio and bulk Pu/U for TMI.

4. CONCLUSIONS

Currently, the only NDA technique that directly measures Pu in SNF involves XRF measurements. Measurements and simulations were used to demonstrate that with a properly

configured detector system, it is feasible to measure the Pu/U atom ratio at the surface of a fuel pin using measurements of the 103.7 keV K X-ray from Pu. Since the Pu/U atom ratio at the surface of the pin is directly related to the average Pu/U concentration for the pin, the technique might be applicable to measuring the Pu/U concentration in an LWR spent fuel pin. However, the technique requires knowledge of the fuel pin design and operating history to properly correlate surface Pu to average Pu for a pin. Fuel history information is available from operator declarations and can be verified by complementary measurements including gamma spectroscopy and passive gross neutron counts.

While the count times of 4 to 12 hours used in these measurements were longer than would be acceptable in most applications, efforts are being made to improve counting time. These include the use of a segmented HPGe detector and reduction of Compton scattering background. These measurements are useful for individual fuel pins and provide a complementary, validating measurement for full assembly techniques.

For future work, optimized detector systems and measurement approaches will be explored with the goal of measuring the Pu/U X-ray ratio with shorter count times. Measurements will be compared with the results of destructive analysis, which is to be completed this year, to provide a correlation between the measured Pu/U ratio and the total Pu/U ratio in the fuel. In addition, the sensitivity of this method to variations in system parameters will be studied to determine the expected accuracy of the technique.

5. REFERENCES

1. P.C. Durst, I. Terios, R. Bean, A. Dougan, B.D. Boyer, R. Wallace, M. Ehinger, D. Kovacic, K. Tolk, *Advanced Safeguards Approaches for new Reprocessing Facilities*, PNNL-16674, U.S. Department of Energy, 2007.
2. Kevin D. Veal, Stephen A. LaMontagne, Stephen J. Tobin, L. Eric Smith, "NGSI Program to Investigate Techniques for the Direct Measurement of Plutonium in Spent LWR Fuels by Non-destructive Assay," Institute of Nuclear Materials Management 51st Annual Meeting, Baltimore, MD, July 11–16, 2010.
3. H. Ottmar, H. Eberle, *The Hybrid K-edge/X-XRF Densitometer: Principles-Design-Performance*, KfK 4590, Kernforschungszentrum Karlsruhe, 1991.
4. Richard W. Ryon, Wayne D. Ruhter, "Uranium and Plutonium Solution Assays by Transmission-Corrected X-Ray Fluorescence Spectrometry," *X-Ray Spectrom.* **28**, 230–232 (1999).
5. C. Rudy, P. Staples, K. Seredniuk, I. Yakovlev, "Determination of Pu in Spent Fuel Assemblies by X-Ray Fluorescence," *Proceedings of the 2005 INMM Annual Meeting*, Phoenix, AZ, 2005.
6. A.S. Hoover, C.R. Rudy, S.J. Tobin, W.S. Charlton, A. Stafford, D. Strohmeier, S. Saavedra, "Measurement of Plutonium in Spent Nuclear Fuel by Self-Induced X-ray Fluorescence," presented at Institute of Nuclear Materials Management 50th Annual Mtg., Tuscon, AZ, July 12–16, 2009.

7. William S. Charlton, Daniel Strohmeyer, Alissa Stafford, Steve Saavedra, Andrew S. Hoover, Cliff Rudy, "The Use of Self-Induced XRF to Quantify the Pu Content of PWR Spent Nuclear Fuel," presented at 31st ESARDA Annual Meeting, Vilnius, Lithuania, May 26–28, 2009.
8. S.F. Saavedra, W.S. Charlton, A.A. Solodov, M.H. Ehinger, "Using NDA Techniques to Improve Safeguards Metrics on Burnup Quantification and Plutonium Content in LWR SNF," presented at Institute of Nuclear Materials Management 51st Annual Mtg, Baltimore, MD, July 11–15, 2010.
9. Alissa S. Stafford, *Spent Nuclear Fuel Self-Induced XRF to Predict Pu to U Content*, Master's Thesis, Texas A & M University, College Station, TX, August 2010.
10. D.B. Pelowitz et al., *MCNPX 2.7A Extensions*, LA-UR-08-07182, Los Alamos National Laboratory, 2008.
11. *Management and Disposition of Excess Weapons Plutonium: Reactor-Related Options*, Panel on Reactor-Related Options for the Disposition of Excess Weapons Plutonium, National Research Council, National Academy Press, Washington, D.C., 1995.
12. D. Reilly, N. Ensslin, and H. Smith, *Passive Nondestructive Assay of Nuclear Materials*, United States Nuclear Regulatory Commission, Washington, DC, NUREG/CR-5550, 1991.
13. *Summary Report of Commercial Reactor Criticality Data for Three Mile Island Unit 1*, TDR-UDC-NU-000004 Rev 01, Bechtel SAIC Company, Las Vegas, 2001.
14. C. Willman, A. Hakansson, O. Osifo, A. Backlin, S.J. Svard, "Nondestructive Assay of Spent Nuclear Fuel with Gamma-Ray Spectroscopy," *Annals of Nuclear Energy* **22**, 427–438 (2006).
15. *TransFX Computer Software Manuals: Advanced Particle Transport Software Using Three-Dimensional Deterministic Methods in Arbitrary Geometry*, Transware Enterprises, 2001.